EFFICIENT CGM APPLICATION FOR SCATTERING AND RADIATION OF ANTENNAS ON BOARD ARBITRARY STRUCTURES

*Olga M. Conde *, Manuel F. Cátedra ***

* Dep. Ingeniería de Comunicaciones. Universidad de Cantabria.
Avda.Los Castros s/n. 39005 Santander (Spain)
Phone: +34 942 201391 (x.21) Fax: +34 942 201873 e-mail: olga@gsr.unican.es

** Dep. Teoría de la Señal y Comunicaciones. Universidad de Alcalá.
Campus Universitario. Ctra. Madrid-Barcelona, km.33,6. 28871 Alcalá de Henares. Madrid (Spain)
Fax: +34 91 8854804 e-mail: felipe.catedra@alcala.es

ABSTRACT

A technique based on an iterative scheme and a current-based method has been developed to determine the scattering and propagation characteristics of arbitrary structures and environments. To obtain a high degree of accuracy, parametric surfaces (NURBS) have been used to model the body surface. The technique solves the MFIE (Magnetic Field Integral Equation) defined over the body surface. The aim of the method is to make the analysis avoiding the memory and CPU time restrictions imposed by low frequency methods such as Method of Moments. Approximate expressions, based on dipole moment formulations, are applied to speed-up the calculations. Two initial guesses for the CGM (Conjugate Gradient Method) have been compared in order to see which one presents the best relationship between convergence and CPU time. Results are presented showing the behavior of the developed methods comparing them with measurements and other electromagnetic methods.

1. INTRODUCTION

The development of a method able to estimate the influence of arbitrary shaped structures on electromagnetic problems has great interest when aspects such as time and money savings are considered. In the application field of on-board antenna design, it is essential to determine the influence of the structure on the radiation pattern of the antenna.

Traditionally, when the electromagnetic influence of a structure had to be determined, one could follow two kinds of electromagnetic procedures: integral rigorous approaches or asymptotic techniques. *Integral rigorous techniques* (Method of Moments (MM) [1], Finite Element method (FE) [2] and Conjugate Gradient-Fast Fourier Transform (CG-FFT) [3]) provide reliable results but they are strongly limited by computer requirements (memory and CPU time) as the frequency of analysis increases. This fact is due to the computation and storage of the mutual impedance matrix. On the other hand, with *Asymptotic techniques* (Geometrical Optics-Uniform Theory of Diffraction (GO-UTD) [4], Physical Theory of Diffraction (PTD) [5], etc.) some propagation features on arbitrary shaped bodies are still not solved. Therefore, the necessity of new techniques capable of obtaining results as exact as the integral rigorous techniques with the computer requirements (low CPU times and memory) associated with the asymptotic ones is obvious. These techniques tend to combine both kinds of methods under a hybrid, iterative or hybrid-iterative structure.

Electromagnetic techniques can also be classified in terms of field-based or current-based methods. The former makes use of intensive ray tracing that can be very cumbersome when arbitrary structures have to be studied, representing one of the main problems of high-frequency methods such as GO-UTD. Current-based methods avoid this ray tracing; they estimate the current on the surface of the structure. The current is represented by means of basis functions.

Focusing on current-based methods, two kinds of integral equations can be solved: the EFIE (Electric Field Integral Equation) and the MFIE (Magnetic Field Integral Equation). Each integral equation enforces different boundary conditions on the structure: in the EFIE, the total tangential electric field on a perfectly electric conductor (PEC) surface is zero and the MFIE enforces the boundary condition on the tangential components of the magnetic field. The EFIE is applicable to both open and closed bodies. Once the integral equation is formulated and solved, the current is obtained and the characterization of the structure (radiation patterns, RCS - Radar Cross Section, etc.) is made straight away.

Looking at literature, one can find hybrid methods that combine integral rigorous techniques with asymptotic ones. As it has been said previously, the main motivation is to reduce the memory and execution time requirements when electrically large structures are analyzed. Some hybrid methods based on the EFIE divide the surface into several regions. The current in each area is calculated following different procedures with the idea of restricting as much as possible the region where the

MM has to work. Generally, the MM region has to include the discontinuities and the transition region between the illuminated and shadowed parts of the structure. Jacobus and Landstorfer [6]-[8] combine PO currents for the illuminated region and MM currents for transition and shadowed areas. Different terms have been added to improve the PO current to account for edges effects of flat plates [6],[7] and straight wedge effects [8] through the introduction of diffraction coefficients derived from UTD.

Within the set of current-based methods, in [9]-[11] Thiele *et al.* present different iterative and hybrid methods to solve the problem of scattering due to plane wave excitation. In [9] the Hybrid Diffraction Technique HDT is presented. In HTD, the surface is split into two regions: the transition region, or MM region, and asymptotic region where the MFIE is directly implemented. The PO current is corrected by some factors. These factors are calculated via MM (MM region) or by coupling calculation (asymptotic region). In [10] the Iterative Method IM is introduced. The IM is a purely iterative method where the induced current is obtained after four iteration processes. These processes find the optical and the correction currents for the illuminated and shadowed regions. Finally in [11] the Hybrid Iterative Method HIM is developed. This technique complements the IM and it takes into account initial currents for the shadow region coming from wedge theory and Fock currents. Recently, Rahmat-Shamii *et al.* [12] have presented their hybrid method HEM (Hybrid EFIE-MFIE). The term hybrid is owed to the resolution of both integral equations EFIE and MFIE on different regions of the geometry. The process is also based on an iterative algorithm. This last method attempts to overcome the difficulties of analyzing structures with open and closed regions. For a wide review of hybrid methods see [13].

The method presented in this paper is a current-based iterative method that formulates the MFIE to find out the electrical induced current on a perfectly conducting structure with arbitrary shape. The main goal of the method is the analysis of closed structures for which the employment of the MFIE is justified. The excitation can be either plane wave or due to an on-board antenna. The MFIE operator is evaluated applying approximated expressions for the mutual impedance matrix derived from previous works. These expressions represent each current basis function in terms of *dipole moments*. The dipole moments reduce the CPU time in the coupling factor calculation. This fact makes their storage unnecessary giving rise therefore to a reduction of memory.

The structure, modeled in 3D, can be completely arbitrary. This degree of flexibility can be obtained with the representation of the environment in terms of parametric surfaces denominated Non-Uniform Rational B-Spline (NURBS) frequently used in the Computer Aided Geometric Design (CAGD) field. The main advantage is that the electromagnetic method works on the model directly collected from the designing process (aeronautical, civil engineering) of the structure and no conversion programs are required. This fact implies that no representation error would be added since the geometry is analyzed as it is.

The same iterative process with different initial conditions has been implemented in order to find which one achieves the best convergence expending the lowest CPU time. The method is based on an algorithm that follows the Conjugate Gradient Method (CGM). A functional is defined over the surface of the structure using the MFIE. The aim of the method is to minimize that functional so, at each iteration, the current is modified to achieve this purpose. When a maximum allowed error is reached, the iteration process stops, and the structure can be characterized by means of its current. The two versions differ in the fact that one of them starts from the PO solution for the initial induced current; in this sense, the method could be considered as hybrid. The main application field is the study of structures whose size is within the resonance range or slightly above. In this area, the MM is limited by computer requirements such as the memory needed to store the matrix elements. The method presented in this paper will only be conditioned by the time needed to calculate the couplings as the frequency gets higher because the number of rooftops-dipole moments increases proportionally to $(\lambda/8)^2$. This problem can be overcome using parallel programming in the coupling factor calculus.

This paper is organized as follows: Section II gives a brief description of how the structure, the excitation and the current are represented. Section III relates to the iterative algorithm followed to solve the problem. Section IV shows different results obtained for canonical structures such as cubes and spheres or arbitrary shaped structures such as airplanes. Results are compared with other electromagnetic methods such as MM and measurements. Finally Section V outlines the conclusions of this work.

2. STRUCTURE, EXCITATION AND CURRENT REPRESENTATION

Apart from the iterative method followed to obtain the current, other important features are:

- geometrical representation of the structure
- excitation characterization
- approximated expressions to represent the current on the surface of the structure

2.1. Geometrical representation

The 3D structures to be analyzed can be completely arbitrary. They are modeled with a set of parametric surfaces called NURBS (Non-Uniform Rational B-Spline) [14]. These modeling were first used in the automotive and aeronautical designing field. Later, and due to their suitable characteristics, they were introduced in the electromagnetic analysis field [15]-[17] because they represent, in a highly accurate way, the real shape of the objects. The main motivation to choose this representation is the fact that the electromagnetic method works directly with the real model and a small set of data is required. Another point to highlight is that flat and canonical surfaces are special issues of NURBS so it can be said that this representation is a high compact model to describe an arbitrary body.

Briefly, a NURBS is a surface which depends on two parametric variables *(u , v)*. The relationship with them is by means of polynomial functions called B-Spline bases. As the B-Spline bases are numerically non-stable, NURBS surfaces are translated into a Bèzier format. Bèzier surfaces are also parametric patches depending on the variables *(u , v)*. In this case, the polynomial functions are Berstein basis. The rest of parameters used to define a Bèzier surface are:

- *parameters (u , v)* : for each surface they take values on the interval [0,1]. So, for each dimension, the value is 0 at one of the surface extremes, and 1 at the opposite one. Each dimension has a polynomial order denoted by m for u and n for v, i.e. for planar surfaces, the order in both dimensions is 2

- *control points* $\vec{p}_{ij}$: in a surface (two dimensions), they form what is denominated as control mesh or control network; this mesh provides an idea of how the surface is. According to the geometric interpretation, the control mesh is the convex hull of the surface. The vertices of the control mesh lie directly on the real surface. These points are given by means of their rectangular coordinates

- *weights* w_{ij} : there is a weight for each control point, they are also called shape parameters because they give an idea of how the real surface approaches control point.

A point on a Bèzier surface, of order m and n, at parametric coordinates *(u , v)* is calculated following (1):

$$\vec{r}(u,v)=\frac{\sum_{i=0}^{m}\sum_{j=0}^{n} w_{ij}\,\vec{p}_{ij}\,B_i^m(u)B_j^n(v)}{\sum_{i=0}^{m}\sum_{j=0}^{n} w_{ij}\,B_i^m(u)B_j^n(v)} \tag{1}$$

where $B_i^m(u)$ and $B_j^n(v)$ are the Bernstein polynomials for each dimension defined as (2):

$$B_i^m(u)=\binom{m}{i}u^i(1-u)^{m-i}$$
$$B_i^m(u)=\frac{m!}{i!\;(m-i)!}u^i(1-u)^{m-i} \tag{2}$$

As an example of a NURBS geometry we have Fig. 1. This drawing represents an airplane constructed with 58 NURBS surfaces. The analysis of this structure will be shown later, in Results Section. For a wide review of NURBS characteristics and properties see [14].

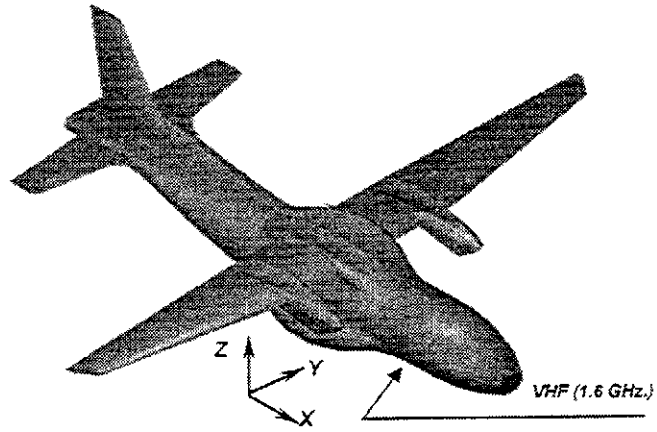

Figure 1.- Example of an airplane modeled with 58 NURBS. VHF antenna is under the airplane.

2.2. Excitation characterization

The excitation of the structure can be by a plane wave as well as by an on-board antenna. The antennas can be modeled with a combination of infinitesimal electric dipoles *IED* and

infinitesimal magnetic dipoles *IMD* [18]. After an empirical process, the number and kind of dipoles, their locations and their dipole moments ($I_o \cdot l$) can be determined in such a manner that the selected dipoles set is able to generate a radiation pattern equivalent to any commercial antenna. Another option could be the direct introduction of the antenna radiation pattern as it is defined by the manufacturer. On the other hand, plane wave excitation is introduced for RCS calculations. For all the excitations, monochromatic time variation $e^{j\omega t}$ is assumed.

2.3. Current representation

As in low frequency methods (MM, CGM), the current is described as a combination of basis functions over the surface of the structure. The basis functions are those developed in [19]. These functions are a generalization of the planar rooftop functions introduced by Glisson [20] but with the peculiarity of being directly defined over the parametric subpatches resulting from the automatic subdivision of surfaces. Each rooftop is defined between two subpatches, as shown in Fig. 2, keeping in mind that the size of each one does not exceed the typical limit of λ/8-λ/10 to realize the variations in current phase. The goal of the iterative method, as in the MM, is to determine the coefficient I_i of each basis function. These coefficients represent the electric current in amperes carried by each rooftop.

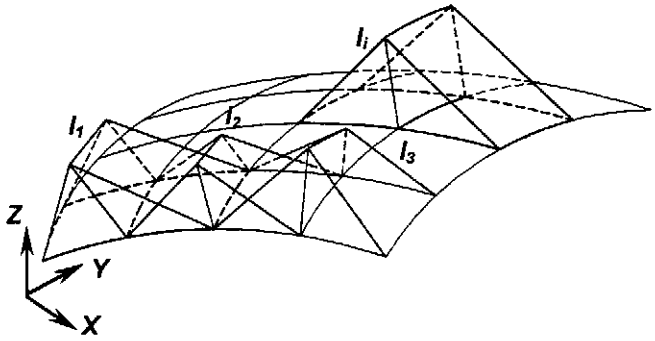

Figure 2.- Current density representation by means of rooftop basis functions.

To compute the field created by this current, *dipole moments approximation* [21] is applied. Under this approximation, a vector with a specific value and orientation substitutes each current rooftop. These vectors, called *dipole moments*, are calculated from the current rooftops described previously. Two kinds of moments can be used: electric dipole moments $\vec{p}$ and magnetic dipole moments $\vec{m}$. Vectors $\vec{p}$ are the most significant when we are dealing with current that presents non-null divergence, as occurs with non quasi-static approaches. In such cases, vector $\vec{m}$ is negligible.

As [21] demonstrates, the dipole moments formulation appears under the simplification of the Green function in free space when far field conditions are assumed. From a computational viewpoint, this approximation is very important because, as Section III shows, simple cross products can substitute the integrals involved in the electromagnetic operators.

3. ITERATIVE METHODS

The method assumes that the surfaces to be analyzed are perfectly electric conductors. From our experience, the on-board antenna problem is related to the analysis of closed bodies of electrically large dimensions. Under this supposition, it is well known [22] that the magnetic field within a perfectly electric conductive structure is zero. In such cases, the MFIE (Magnetic Field Integral Equation) is a good choice to find the induced current on the surface of the body. Besides the initial goal of closed structures analysis, we have also observed some reliable radiation pattern results when the MFIE has been applied to non-closed structures with large electrical dimensions; this article presents a significant case of this last fact.

So, the MFIE yields to the expression (3):

$$\hat{n} \times \vec{H}^{total}(\vec{r}) = 0$$
$$\hat{n} \times \left(\vec{H}^{imp}(\vec{r}) + \vec{H}^{scatt}(\vec{r})\right) = 0 \qquad (3)$$

where $\vec{r}$ is located under the surface. The position above or under the surface is discriminated by means of the outgoing normal vector $\hat{n}$. In expression (3), $\vec{H}^{imp}$ relates to the magnetic field impressed by the external sources (plane waves or infinitesimal dipoles) and $\vec{H}^{scatt}$ is the magnetic field radiated by the induced electric current on the body's surface $\vec{J}$. The expression for $\vec{H}^{scatt}$ will be an operator directly applied to the current $\vec{J}$; this operator is denoted as $L_H[\vec{J}]$.

If we return to the expression (3), we can see that it represents a minimization problem where the solution is more

valid, the closer the expression is to zero. This fact makes us choose an algorithm capable of finding the current $\vec{J}$ that accomplishes with that expression. We have followed a CGM (Conjugate Gradient Method) [23]. The CGM algorithm is based on the minimization of a functional defined over a variable, in our case $\vec{J}$. The functional is related to the error in expression (3) and it is defined as:

$$Functional\ (\vec{J}) = \langle \vec{e}, \vec{e} \rangle = \|\vec{e}\|^2$$
$$\vec{e} = \hat{n} \times \left(\vec{H}^{scatt} + \vec{H}^{imp} \right) \tag{4}$$

where $\langle \cdot \rangle$ indicates inner product, $\| \cdot \|$ stands for vector norm and $\vec{e}$ denotes the residual in CGM nomenclature.

We have to be very careful in the selection of the $\vec{H}$ sign. As it is evaluated within the structure, it has the opposite sign than the one evaluated in the exterior. The evaluation of $\vec{H}$ is done by the application of the appropriate operator, $L_H[\vec{J}]$, over the current:

$$\vec{e} = \hat{n} \times \left(\vec{H}^{imp} + \vec{H}^{scatt} \right)$$
$$\vec{e} = \hat{n} \times \left(\vec{H}^{imp} + L_H[\vec{J}'] \right) \tag{5}$$

where $\vec{J}'$ is the approximate solution for $\vec{J}$.

The iterative method starts with an initial guess for $\vec{J}$, namely $\vec{J}_0$ that is made null, and afterwards it progresses following the algorithm [23] till the required relative error is achieved in (5). The relative error after k th-iteration is evaluated following:

$$\varepsilon^{(K)} = \frac{\left\| \hat{n} \times \left(\vec{H}^{imp} + L_H[\vec{J}^{(K)}] \right) \right\|}{\left\| \hat{n} \times \vec{H}^{imp} \right\|} < \varepsilon_{max} \tag{6}$$

where $\vec{J}^{(K)}$ is the induced electric current density after k th-iteration. The stop condition is also included in expression (6), that is, the error should be less than a specified value ε_{max}, typical values for the error are 0.01 or 0.001.

The next step in the method description is the definition of the operator $L_H[\vec{J}]$. This operator obtains the magnetic field $\vec{H}$ due to the current $\vec{J}$ as expression (7) shows:

$$L_H[\vec{J}] = \frac{1}{4\pi} \int_S \vec{J}(\vec{r}') \times \nabla' G(\vec{r}, \vec{r}')\ ds' \tag{7}$$

where $G(\vec{r}, \vec{r}')$ is the Green's function in vacuum defined as:

$$G(\vec{r}, \vec{r}') = \frac{e^{-jk|\vec{r}-\vec{r}'|}}{|\vec{r}-\vec{r}'|} \tag{8}$$

where $k = 2\pi/\lambda$ is the vacuum wavenumber with λ the wavelength; $\vec{r}$ and $\vec{r}'$ are the observation and source points, respectively.

If the Green's function is differentiated with respect to the primed coordinates, we have the expression (9):

$$L_H[\vec{J}] = \frac{-1}{4\pi} \int_S \left(\frac{1 + jk|\vec{R}|}{|\vec{R}|^3} \right) e^{-jk|\vec{R}|} \left[\vec{R} \times \vec{J}(\vec{r}') \right] ds'$$
$$\vec{R} = \vec{r} - \vec{r}' \tag{9}$$

Expression (9) involves several integrals because of the cross product within the integral. It is obvious that if each coupling factor is evaluated with (9), when the electric size of the structure is high, we are in front of a tedious computational problem. Usually, as coupling calculation is highly time consuming, the coupling factors are calculated once and then they are stored for a later manipulation. When dipole moments approximation is taken into account, a simple cross product substitutes the complicated integral. With this operation, the coupling evaluation is very fast and there is no need for storage.

The magnetic field induced on rooftop i due to a current located at rooftop j applying the electric dipole moment $\vec{p}_j$ is shown in (10):

$$L_i[\vec{J}_j] \approx \frac{e^{-jk|\vec{R}|}}{4\pi|\vec{R}|^2}\left(\frac{1}{|\vec{R}|}+j\sqrt{\omega^2\mu\varepsilon}\right)I_j(\vec{p}_j\times\vec{R}) \qquad (10)$$

$$\vec{R}=\vec{r}_i-\vec{r}_j,\ \forall i\neq j$$

where μ and ε are free space permeability and permittivity, respectively. The vector $\vec{p}_j$ relates to the electric dipole moment of the current density in the rooftop j. The expression for $\vec{p}_j$ is (11):

$$\vec{p}_j=\int_{S_j}\vec{J}_j(\vec{r}')\,ds' \qquad (11)$$

where S_j is the surface area subtended under rooftop j, i.e. the area of two subpatches.

The magnitude applied to each dipole moment, I_j, is calculated at each iteration as the Conjugate Gradient algorithm states. After the calculation of $L_i[\vec{J}_j]$, the magnetic field is averaged over rooftop i applying as a testing function, the one shown in Fig. 3. The testing function of a subdomain is defined along the boundary line between the two subpatches over which the subdomain extends. The testing functions we introduce look like curved *'razor-blades'*. However, it must be noticed that the testing functions we are considering are 'approximately' perpendicular to the ones typically used in the EFIE formulations. In our approach for the MFIE we are considering a 'razor-blade' transversal to the subdomain current, while in the EFIE formulation, the 'razor-blade' is defined parallel to the subdomain current. In Fig. 3 the current flows from subpatch 1 to subpatch 2. Considering the current parallel to the u coordinate, we have the following expression for the testing function:

$$W_i(u,v)=\begin{cases}1 & if\ v_{min}\le v\le v_{max}\\ 0 & elsewhere\end{cases} \qquad (12)$$

where v_{min}, v_{max} are the minimum and maximum limits for the parametric coordinate v of subpatches 1 and 2.

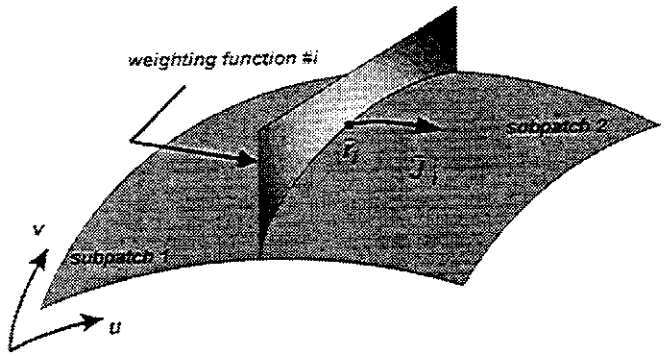

Figure 3.- Testing function defined along the subpatches boundaries.

Expression (10) becomes singular for $\vec{r}_i=\vec{r}_j$. This situation appears when the field induced by the own current of a subdomain has to be evaluated. At this point, the operator $L_H[\vec{J}]$ when $\vec{r}=\vec{r}$ is formulated as:

$$L_i[\vec{J}_i]\approx-\frac{1}{2}\vec{J}_i\times\hat{n}_i \qquad (13)$$

where $\vec{J}_i$ is the current density on rooftop i and $\hat{n}_i$ is the unitary outgoing normal vector at $\vec{r}_i$.

An important step in the Conjugate Gradient algorithm is the definition of the adjoint operator of $L_H[\vec{J}]$, denoted by $L_H^{adj}[\vec{J}]$. The adjoint operator over rooftop i due to the current at $\vec{r}_j$ is computed as:

$$L_i^{adj}[\vec{J}_j]=\frac{e^{-jk|\vec{R}|}}{4\pi|\vec{R}|^2}\left(\frac{1}{|\vec{R}|}+j\sqrt{\omega^2\mu\varepsilon}\right)I_j(\vec{p}_i\times\vec{R}')^* \qquad (14)$$

$$\vec{R}'=\vec{r}_j-\vec{r}_i,\ \forall i\neq j$$

where $(\ )^*$ stands for complex conjugate. When $\vec{r} = \vec{r}_j$, the adjoint operator is:

$$L_i^{adj}[\vec{J}_i] = -\frac{1}{2}\left(\vec{J}_i \times \hat{n}_i\right)^* \tag{15}$$

For our application, the Conjugate Gradient algorithm [23] begins to iterate with a null current, that is, all coefficients I_i are set to zero. Later, and as a function of the impressed fields, the current is modified at each iteration, changing the coefficients I_i. The method stops when condition (6) is satisfied.

Once the induced current has been calculated, the radiated electric field $\vec{E}^{scatt}$, under far field conditions, can be evaluated. For this task, the electric dipole moments $\vec{p}$ are also utilized [21]:

$$\vec{E}^{scatt}(\hat{s}) = \frac{-j\omega\mu}{4\pi} \sum_{i=1}^{N^o\ rooftops} I_i \left[\vec{p}_i - (\hat{s}\cdot\vec{p}_i)\hat{s}\right] e^{jk(\vec{r}_i\cdot\hat{s})} \tag{16}$$

where $\hat{s}$ is the observation direction.

The iteration procedure is completely defined, next step will be the characterization of the two versions derived from the Conjugate Gradient algorithm. They differ in what is considered as impressed field, $\vec{H}^{imp}$, in the definition of the functional (5).

3.1. CGM # 1

In this case, the impressed magnetic field $\vec{H}^{imp}$ is the field directly due to the external sources. From now on, this external field will be denoted as $\vec{H}^{ext}$. The induced current, given as solution, is the one obtained when the Conjugate Gradient algorithm achieves the required error.

$$\vec{H}^{mp} = \vec{H}^{ext} \quad \Rightarrow \quad \vec{J} = \vec{J}^{CGM} \tag{17}$$

3.2. CGM # 2

In CGM#2, the impressed magnetic field $\vec{H}^{mp}$ is both the one due to the external sources, $\vec{H}^{ext}$, and the one that $\vec{J}^{PO}$ induces. $\vec{J}^{PO}$ is the *Physical Optics* approximation current, i.e. current is calculated only on the illuminated region of the geometry as Fig. 4 illustrates.

$$\vec{J}^{PO}(\vec{r}) = \begin{cases} 2\hat{n}\times\vec{H}^{ext}(\vec{r}) & \vec{r}\in S^{illuminated} \\ 0 & \vec{r}\in S^{shadowed} \end{cases} \tag{18}$$

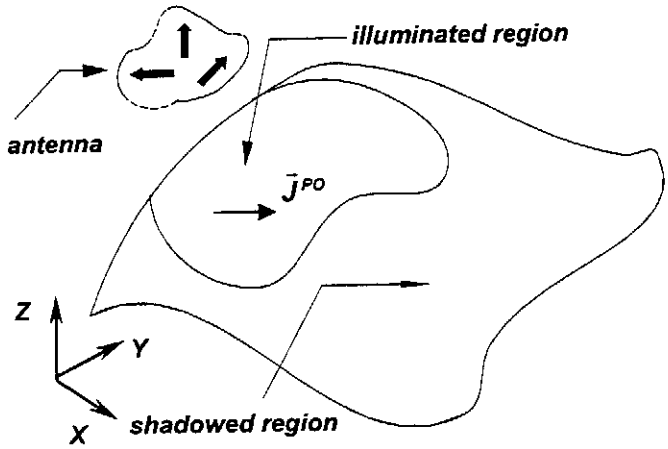

Figure 4.- Physical Optics approximation for the current.

The current obtained with the iterative method, $\vec{J}^{CGM}$, will be now a residual current. $\vec{J}^{CGM}$ corrects the PO current on the illuminated region of the structure, and it is directly the induced current on the shadowed region because there, $\vec{J}^{PO}$ is null.

$$\vec{H}^{imp} = \vec{H}^{ext} + L_H[\vec{J}^{PO}] \Rightarrow \vec{J} = \vec{J}^{PO} + \vec{J}^{CGM} \tag{19}$$

4. RESULTS

This section will show some results concerning both canonical structures and realistic targets. Results of the iterative methods are compared with measurements as well as with MM computation [19]. Perfectly conducting surfaces are considered

in all cases. The iterative methods have been implemented in a Fortran code called *SIMCOR*. Table I illustrates the efficiency achieved with respect to an MM code and to a PO code. In order to have a proper reading of Table I, the MM and SIMCOR results have been obtained considering a maximum allowed error ε_{max} of 0.01, expression (6). The computer used is a Silicon Graphics PowerChallenge (size L) with 1Gbyte of RAM and 1 processor R10000 has been used, this processor can reach a peak performance of 380 MFlops.

	Number Rooftops	MEMORY (Mbytes)	
		MM	SIMCOR
CUBE	1452	49.2	**1.2**
CYLINDER-PLATE	4643	448.5	**1.6**

	CPU TIME			
	MM	PO	CGM#1	CGM#2
CUBE	00:11:52	00:00:01	00:05:59 (13 it)	00:06:53 (15 it)
CYLINDER-PLATE	02:35:22	00:00:16	00:44:54 (10 it)	00:59:19 (13 it)

Table I .- Performance of the developed methods. Computer resources: memory and CPU time.

4.1. Cube

Fig. 5 shows a cube with side of λ. A cube side of λ, total surface of 6 λ^2, needs 1452 basis functions if we consider 10 rooftops per wavelength. The excitation is an infinitesimal electric dipole located above the top face of the cube at a height of λ/2. The dipole moment for the antenna $I_0 \cdot l$ is 1.0 and its orientation respect to the absolute coordinate system is $\theta_{dip} = 90°$, $\varphi_{dip} = 45°$. The dipole is shifted from the center of the top face towards the vertex and it is separated 0.1 λ from the vertex. The radiation pattern for the far field, E_θ component at the cut $\varphi = 0°$, is shown in Fig. 6. The main comments to be made are that both versions of the CG algorithm converge on the same value and they are really close to the MM solution. A great improvement is obtained with respect to the PO solution (dashed line). The dipole has been located so near the vertex to consider its effect, as Fig. 6 shows, the behavior of the new method is satisfactory in the analysis of such kind of discontinuities.

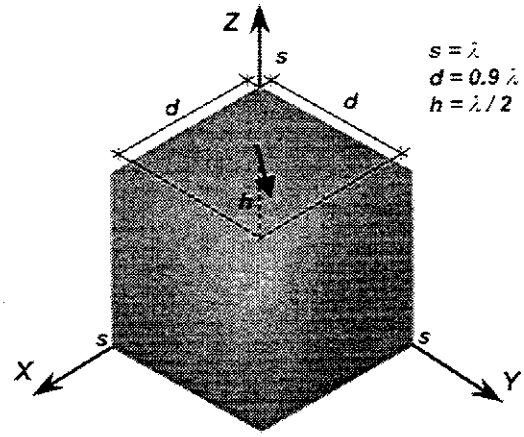

Figure 5.- Cube geometry, the side of the cube is 1 λ. The arrow indicates the position of an infinitesimal electric dipole considered as the external excitation.

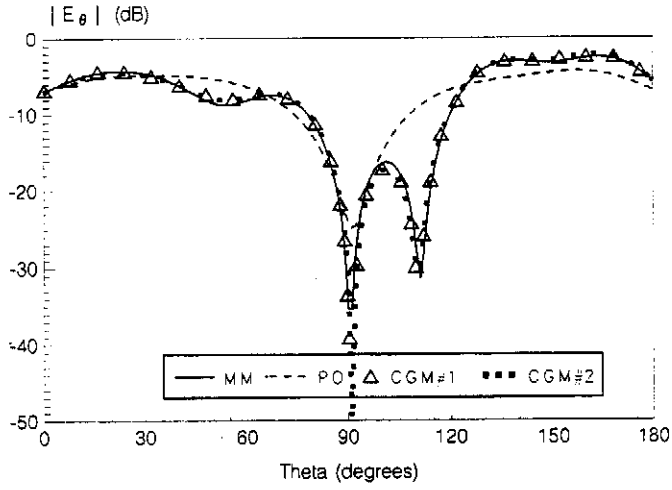

Figure 6.- Far field radiation pattern for the cube, E_θ component, cut $\varphi = 0°$.

4.2. Cylinder-Plate

In this case, an open structure is studied, Fig. 7. This geometry is composed of a quarter of a cylinder (radius=3λ, length=3λ) and an attached plate of dimensions 3λ × 4.5λ. The

infinitesimal electric dipole is located at 1.5λ from one side of the plate at a height of λ/2. The area to analyze is bigger, 27.6 λ^2 which requires 4643 unknowns (8/λ in the curved surface and 10/λ in the plate). Fig. 8 presents the radiation pattern for the E_θ component in the cut $\phi = 90°$. Unexpected reliable results are obtained except for the deep shadow regions, but here the field magnitude is 30 dB below the maximum value. An overall improvement with respect the PO solution is again obtained.

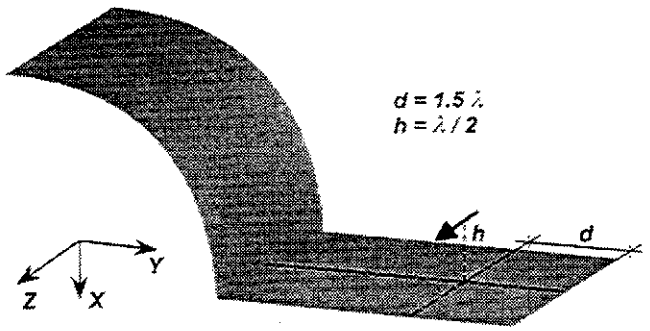

Figure 7.- Cylinder-Plate geometry and position of the infinitesimal electric dipole considered as the external excitation.

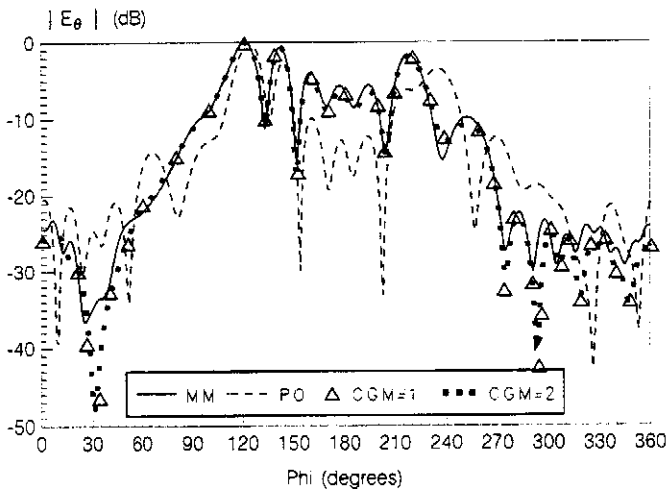

Figure 8.- Far field radiation pattern for the cylinder-plate, E_θ component, cut $\phi = 90°$.

This good behavior could be explained because the structure is large enough to suppose that the magnetic field under the surface is very small. In this case, the application of the MFIE is not so erroneous. The committed error is negligible, and apparently, it does not affect the results.

4.3. Airplane

Fig. 1 shows a realistic airplane. The airplane analyzed is a scaled model 1:12 represented by 58 NURBS. SIMCOR results are compared directly with measurements. The on-board antenna is denominated VHF and it is placed under the airplane as Fig. 1 shows. This antenna is a typical blade antenna with hemispherical coverage. The antenna is oriented parallel to Z-axis and positioned at the front part of the fuselage really close to its surface as indicated in the figure. The absolute coordinate system is centered inside the structure. For the operation frequency of the VHF antenna, the airplane dimensions are 9.5λ × 11.4λ × 3.2λ. The number of subdomain basis required for this analysis has been 17770. This problem only requires 5.8 Mbytes of memory RAM. The iterative version CGM#2 has completed 91 iterations to achieve an error of 0.1.

Fig. 9 represents the far field radiation pattern, E_θ component, for the cut $\phi = 90°$. The results for CGM#2 version are shown with a dotted line, the PO solution with a dashed line and the measurements with a continuous line. Really good approximation to the measurements can be observed and an appreciable improvement with respect PO solution is also obtained.

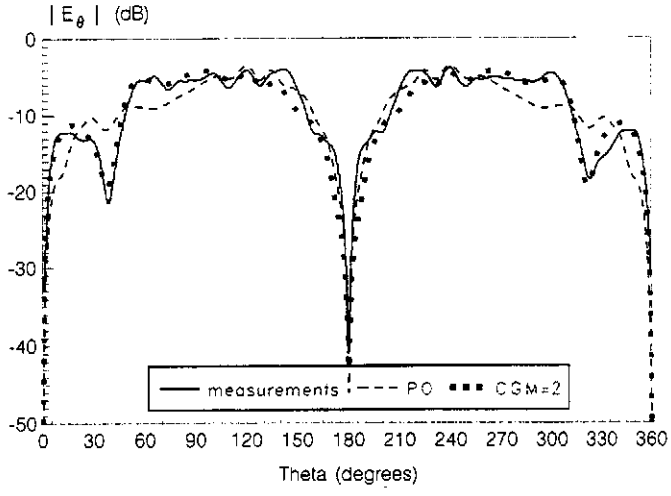

Figure 9.- Far field radiation pattern for the airplane, E_θ component, cut $\phi = 90°$.

5. CONCLUSIONS

An iterative method has been developed in order to find the induced electric current on the surface of complex 3D structures with arbitrary shape. The structures are modeled using parametric surfaces called NURBS. An important feature of the developed method is the application of the *dipole moments formulation*. Under this approximation, the implementation of the MFIE is done very fast and the coupling matrix is not stored. The efficiency in computer resources, compared with MM requirements, can be observed in the figures shown in Table I.

The iterative scheme is based on the Conjugate Gradient Algorithm. The CG algorithm ensures the convergence for all the tests considered. Two different versions of CG algorithm have been implemented changing the impressed field in the functional definition (5). One of the versions changes this impressed field taking into account the Physical Optics currents, in this sense, the method could be considered as hybrid.

Both iterative versions reach the same solution for the current although one takes a larger number of iterations than the other. This is because the maximum allowed error does not have the same meaning for the two versions. Version *CGM#2* is more accurate for the same value of ε_{max} because the impressed field $\vec{H}^{imp}$ is lower since the field due to the PO currents tries to cancel out the external field due to the excitation.

Finally, the CG algorithm implies the computation of four operators L_H for each iteration so, these methods are appropriate for the analysis of structures with electrical dimensions on the resonance range or slightly above.

ACKNOWLEDGMENTS

This work has been supported by a CYCIT under a FPU grant. Authors are grateful to the CYCIT, Proyecto de Infraestructura IN94-0108 and to the Project TIC: 96-0653. Finally, the authors would like to thank the C.A.S.A Company for the opportunity to work with measurements and realistic models of geometry.

REFERENCES

[1] R.F.Harrington, *Field Computation by Moment Methods*, McMillan, New York, 1968.

[2] M.A.Morgan, "Principles of finite methods in electromagnetic scattering" in *Finite Element and Finite Difference Methods in Electromagnetic Scattering* , (PIER 2 of Progress in Electromagnetic Research series), J.A.Kong, Ed. Elsevier, Ch.8, pp.287-373, 1990.

[3] M.F. Cátedra, R.P. Torres, J. Basterrechea, E.Gago, *'The CG-FFT Method. Application of Signal Processing Techniques to Electromagnetics'*, Artech House Inc., Boston, 1995.

[4] D.A.McNamara, C.W.I.Pistorius, J.A.G.Malherbe, *Introduction to the Uniform Geometrical Theory of Diffraction*, Artech House Inc., Norwood, 1990.

[5] E.F.Knott, "A Progression of High-Frequency RCS Prediction Techniques", *Proceedings of IEEE*, Vol.73, No.2, pp.252-264, February 1985.

[6] U.Jakobus, F.M.Landstorfer, "Improved PO-MM Hybrid Formulation for Scattering from Three-Dimensional Perfectly Conducting Bodies of Arbitrary Shape", *IEEE Trans. on Antennas and Propagation*, Vol.43, No.2, pp.162-169, February 1995.

[7] U.Jakobus, F.M.Landstorfer, "Current-Based Hybrid Moment Method Analysis of Electromagnetic Radiation and Scattering Problems", *ACES Journal: Special Issue on Advances in the Application of the Moment Method to Electromagnetic Radiation and Scattering Problems*, Vol.10, No.3, pp.38-46, 1995.

[8] U.Jakobus, F.M.Landstorfer, "Improvement of the PO-MoM Hybrid Method by Accounting for Effects of Perfectly Conducting Wedges", *IEEE Trans. on Antennas and Propagation*, Vol.43, No.10, pp.1123-1129, October 1995.

[9] T.J.Kim, G.A.Thiele, "A Hybrid Diffraction Technique: General Theory and Applications", *IEEE Trans. on Antennas and Propagation*, Vol.30, No.5, pp.888-897, September 1982.

[10] M.Kaye, P.K.Murthy, G.A.Thiele, "An Iterative Method for Solving Scattering Problems", *IEEE Trans. on Antennas and Propagation*, Vol.33, No.11, pp.1272-1279, November 1985.

[11] P.K.Murthy, K.C.Hilll, G.A.Thiele, "A Hybrid-Iterative Method for Scattering Problems", *IEEE Trans. on Antennas and Propagation*, Vol.34, No.10, pp.1173-1180, October 1986.

[12] R.E.Hodges, Y.Rahmat-Samii, "An Iterative Current-Based Hybrid Method for Complex Structures", *IEEE Trans. on Antennas and Propagation*, Vol.45, No.2, pp.265-276, February 1997.

[13] G.A.Thiele, "Overview of Selected Hybrid Methods in Radiating System Analysis", *Proc. IEEE*, Vol.80, No.1, pp.67-78, January 1992.

[14] G.Farin, *'Curves and Surfaces for Computer Aided Geometric Design, A Practical Guide'*, Academic Press Inc., London, 1988.

[15] D.M.Elking, S.D.Alspach, D.D.Car, K.E.Castle, J.L.Karty, J.H.Knebans, R.A.Perlman, J.M.Roedder, "Electromagnetic Analysis Codes", *IEEE Antennas and Propagation International Symposium*, Chicago, Vol.3, pp.1306-1309, July 18-25 1992.

[16] T.A.Blalock, "Modern RCS Computations - A Practical Approach", *IEEE Antennas and Propagation International Symposium*, Chicago, Vol.3, pp.1298-1301, July 18-25 1992.

[17] J.Pérez, M.F.Cátedra, "RCS of Targets Modelled with NURBS Surfaces", *IEEE Antennas and Propagation International Symposium*, Chicago, Vol.2, pp.965-968, July 18-25 1992.

[18] M.Domingo, R.P.Torres, M.F.Cátedra, "On Board Antennas Modelled by Using Simple Radiating Elements", *Euro Electromagnetics 94*, ESA, Burdeos, France, May 30-June 4 1994.

[19] M.F.Cátedra, F.Rivas, L.Valle, "A Moment Method Approach Using Frequency Independent Parametric Meshes", *IEEE Trans. on Antennas and Propagation*, Vol.45, No.10, pp.1567-1568, October 1997.

[20] A.W.Glisson, D.R.Wilton, "Simple and Efficient Numerical Methods for Problems of Electromagnetic Radiation and Scattering from Surfaces", *IEEE Trans. on Antennas and Propagation*, Vol.28, pp.593-603, September 1980.

[21] S.Piedra, J.E.Fernández, J.Basterrechea, M.F.Cátedra, "A Quasi-Static Tool for the EMI/EMC Analysis of Analog Circuits: PET+SEP", *IEEE Trans. Electromagnetic Compatibility*, Vol. 40, No. 2, pp. 127-138, May 1998.

[22] C.A.Balanis, *'Advanced Engineering Electromagnetics'*, John Wiley & Sons, New York, 1989.

[23] M.F.Cátedra, J.G.Cuevas, L.Nuño, "Scheme to Analyze Conducting Plates of Resonant Size Using the Conjugate-Gradient Method and the Fast Fourier Transform", *IEEE Trans. on Antennas and Propagation*, Vol.36, pp.1744-1753, December 1988.